

Article

Prediction of Curing Time/Shear Strength of Non-Conductive Adhesives Using a Neural Network Model

Kyung-Eun Min ¹, Jae-Won Jang ¹, Jun-Ki Kim ², Sung Yi ¹ and Cheolhee Kim ^{1,2,*} ¹ Department of Mechanical and Material Engineering, Portland State University, Portland, OR 97201, USA² Welding and Joining R&D Group, Korea Institute of Industrial Technology, 156, Getbeol-ro, Yeosu-gu, Incheon 21999, Republic of Korea* Correspondence: chkim@kitech.re.kr or cheol@pdx.edu

Abstract: Electronic packaging has been developed with high resolution and fine interconnection pitches. Non-conductive adhesives (NCAs) have been growing with the increase of I/O pad count and density, along with fine pad bond pitch interconnections. Prediction and optimization of NCA characteristics are inherently complicated due to various and extensive materials composing NCAs. In this study, a framework predicting the curing time and shear strength of an NCA is established by a neural network model. NCA formulations with 4 resins, 3 hardeners, 8 catalysts, and a coupling agent were selected from in-house experiments, and an artificial neural network (ANN) with one dense layer with 3 nodes was trained using 65 data points. Model accuracy was improved by 28.9–35.2% compared with the reference, and the trained model was also verified through third-party reference data. Prediction of NCA properties and optimization of NCA formulations for mass production were demonstrated by using the trained ANN model. This paper provides a framework for ANN-based NCA design and confirmed the feasibility of ANN modeling, even with a small dataset.

Keywords: neural network; prediction; optimization; non-conductive adhesives; formulation

Citation: Min, K.-E.; Jang, J.-W.; Kim, J.-K.; Yi, S.; Kim, C. Prediction of Curing Time/Shear Strength of Non-Conductive Adhesives Using a Neural Network Model. *Appl. Sci.* **2022**, *12*, 12150. <https://doi.org/10.3390/app122312150>

Academic Editor: Vincent A. Cicirello

Received: 7 October 2022

Accepted: 23 November 2022

Published: 28 November 2022

Publisher's Note: MDPI stays neutral with regard to jurisdictional claims in published maps and institutional affiliations.



Copyright: © 2022 by the authors. Licensee MDPI, Basel, Switzerland. This article is an open access article distributed under the terms and conditions of the Creative Commons Attribution (CC BY) license (<https://creativecommons.org/licenses/by/4.0/>).

1. Introduction

Electronic packaging technology has been developed with the semiconductor industry to offer the functional capability to apply high density and performance [1–3]. Due to the requirement of high resolution and fine interconnection pitch (less than 25 µm), the flip-chip bonding process using adhesives has been also emerged and developed in electronic packaging industries to replace underfill materials, which are widely used in electronic packaging but prone to cause void defects after gap-filling [4].

Adhesives for the flip-chip bonding process are classified as an isotropic conductive adhesive (ICA), an anisotropic conductive adhesive (ACA), and a non-conductive adhesive (NCA) [1]. NCA does not contain conductive fillers and reduces the probability of electric short-circuiting between the fine-pitch or the bump (chip) and the pad (substrate) caused by trapped conductive fillers that are included in ICA and ACA [5]. In addition, a chip and a substrate can directly contact electrically using NCA, therefore the contact area is increased, and then the contact resistance is also reduced [6]. The application of NCA increases as the number of I/O pads and the fine-pitch density of the interconnections increase.

Many researchers have formulated NCA by combining epoxy resin, hardener, catalyst, etc. Epoxy resins are widely used as polymeric adhesives with versatility, good wetting ability, chemical resistance, and high tensile strength. However, epoxy resins have low toughness and weak peeling/impact strength [7,8]. Therefore, epoxy resins are formulated with a hardener and a catalyst to compensate for their disadvantages. Kim et al. [4] showed the reliability of fine-pitch chip-on-film (COF) flip-chip packages using NCA. They evaluated 4 types of curing agents and suggested 2E4MZ-CN as a suitable curing agent for the formulation of NCA in terms of the curing rate and pot life. Min et al. [9] studied the

effects of hardeners and catalysts on the reliability of copper-to-copper adhesive joints. They evaluated 4 types of hardeners and 2 types of catalysts to formulate 6 types of NCAs. Curing behaviors and shear strengths of NCAs were compared, and the optimum formulation with high initial joint strength and reliability was suggested. Recently, Lee et al. [10] investigated epoxy/silane pre-synthesis, which improved thermal properties and adhesion strength. The modified NCA showed 1.45 times higher shear strength than the neat NCA. Inherently, the properties of NCAs depended on the components and their compositions and components [11–15], and formulation of NCA is extremely sophisticated because various kinds of materials are employed as components.

Snap curing time and shear strength are important properties of NCAs to determine productivity in mass production and the reliability of the electronic packages. Snap curing time of NCA should be considered to improve productivity in the flip-chip bonding process, which is to bond between Si chip and substrate one by one [16,17]. Additionally, high-temperature thermo-compression is accompanied by the bonding process, which causes substrate softening and the joint deterioration [18,19]. Therefore, the shear strength for interconnection between a chip and a substrate affects the reliability of the package.

Curing time and shear strength have been experimentally and analytically examined for various NCAs according to their composition. Min et al. [17] reported an evaluation method for snap curing behavior on NCA for flip-chip bonding. They proposed the DEA (dielectric analysis) method for quantitatively investigating snap curing behavior of NCA and verified the DEA method as compared with the results using the isothermal DSC method. Min et al. [20] proposed the effects of four types of catalysts on the curing time of NCA. The curing time was decreased with an increase in the content of catalysts. Yang et al. [21] studied an analytical approach to evaluate shear stress in flip-chip interconnection using NCA. They found the shear stress distribution induced by coefficient of thermal expansion mismatch at the adhesive layer using analytical approaches, such as bonded joint and CBA (Composite Beam Analysis) method.

Since numerous NCAs are formulated using various materials depending on the operating conditions, it is difficult to predict the behavior of NCA due to non-linearity and so characterization has relied on an experimental approach. Recently, machine learning (ML)-based studies have been reported to optimize and predict mechanical properties of adhesive joints. Pruksawas et al. [22] studied the prediction and optimization of the strength of epoxy adhesive joints. Only 32 data points with an epoxy resin and amine curing agent with four different molecular weights were considered. A gradient boosting machine learning model achieved a considerable accuracy with a coefficient of determination (R^2), root mean square error (RMSE), and mean absolute error (MAE) of 0.85, 4.0 MPa, and 3.0 MPa, respectively. However, there are limitations such as the small datasets and consideration of only a few types of materials. Kang et al. [23] showed the prediction of the lap-shear strength of epoxy adhesive using an ANN model. The optimized ANN models for lap-shear strength showed RMSEs of 0.053 and 0.590 and R^2 values of 0.642. However, types of resin, hardener, and catalyst were fixed; consequently, there was a limitation for a variety of materials. Therefore, research for prediction is needed for various material components.

To overcome the current limitations of an experimental approach to characterize NCA, a ML framework considering various and extensive materials was investigated in this study. NCAs were formulated from 4 types of resins, 3 types of hardeners, 8 types of catalysts, and 1 type of coupling agent, and curing time and shear strength were measured by DEA and the die shear test, respectively. ANN models were trained using 65 data points, and the trained ANN models were verified by third-party experimental data from references. The prediction and the optimization for the curing time and shear strength of NCA were demonstrated according to the content of catalyst, hardener, and resin. From the results, a framework for prediction of the curing time/the shear strength of NCA and optimization of the NCA formulations using the ANN models was successfully exhibited.

2. Materials and Methods

2.1. Non-Conductive Adhesives Formulation

In this study, 4 types of resins, 3 types of hardeners, 8 types of catalysts, and a coupling agent were selected. Epoxy resins employed in this study were diglycidyl ether of bisphenol A (DGEBA), diglycidyl ether of bisphenol F (DGEBF), diglycidyl ether of bisphenol F with Novolac (Novolac 160), and 3,4-Epoxy cyclohexylmethyl-3',4'-epoxycyclohexane carboxylate. Hardeners employed were Methylhexahydrophthalic anhydride (MHHPA), tetrahydrophthalic anhydride (THPA), and adipic dihydrazide (ADH). Catalysts employed were novacure (micro-encapsulated imidazole type latent catalyst), imidazole, 2-methylimidazole (2MZ, powder imidazole type catalyst), 2-ethyl-4-methylimidazole (2E4MZ), 1-Cyanoethyl-2-ethyl-4-methylimidazole (2E4MZ-CN), 2,4-diamino-6-[2'-methylimidazolyl-(1')]-ethyl-s-triazine (2MZ-A), dicyandiamide (DICY), and triphenylphosphine. A coupling agent of gamma-methacryloxypropyltrimethoxysilane was used. The chemical properties of NCA ingredients are summarized in Table 1.

Hardeners of MHHPA and THPA were formulated at 1:0.8 of epoxy to hardener equivalent ratio, and ADH hardener was formulated at 1:1 of epoxy to hardener equivalent ratio. Based on the contents of resin and hardener, catalysts were formulated from 5 phr (per hundred resin) to 30 phr, and lastly, 0.55 phr of coupling agent was added.

Table 1. Chemical properties of NCA.

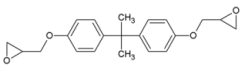
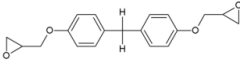
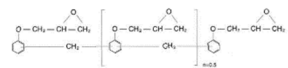
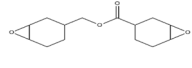
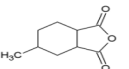
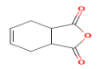
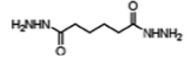
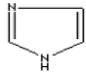
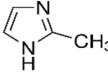
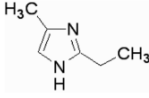
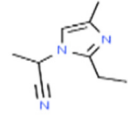
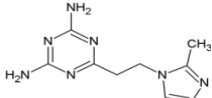
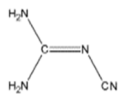
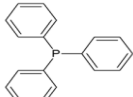
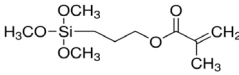
Ingredient	Chemical Name	Abbreviation	Chemical Structure	Molar Mass (g/mol)	Melting Point (°C)
Resin	Diglycidyl ether of bisphenol A	DGEBA		340	8–12
	Diglycidyl ether of bisphenol F	DGEBF		312	−15
	Diglycidyl ether of bisphenol F with Novolac	Novolac 160		168	-
	3,4-Epoxy cyclohexylmethyl 3,4-epoxycyclohexanecarboxylate	ERL 4221		252	250
Hardener	Methylhexahydrophthalic anhydride	MHHPA		168	−30
	Tetrahydrophthalic anhydride	THPA		152	98
	Adipic dihydrazide	ADH		174	180–182

Table 1. Cont.

Ingredient	Chemical Name	Abbreviation	Chemical Structure	Molar Mass (g/mol)	Melting Point (°C)
	Novacure	HX3941	Microencapsulated 2MZ	185	-
	Imidazole	Z		68	88–92
	2-methylimidazole	2MZ		82	137–145
	2-ethyl-4-methylimidazole	2E4MZ		110	41
Catalyst	1-cyanoethyl-2-ethyl-4-methylimidazole	2E4MZ-CN		163	~30
	2,4-diamino-6-[2'-methylimidazolyl-(1')]-ethyl-s-triazine	2MZ-A		219	248–258
	Dicyandiamide	DICY		84	208
	Triphenylphosphine	TPP		262	208
Coupling agent	gamma-Methacryloxypropyl-trimethoxysilane	A-174		248	<−20

2.2. Specimens and Analysis

2.2.1. Curing Time Measurement

In this study, the snap curing time of NCA quantitatively is measured by DEA using a change in the rate of dielectric loss of adhesives as a function of time at a fixed temperature. The curing time measuring equipment consisted of an impedance analyzer, a heating state, and a DEA sensor as shown in Figure 1.

The DEA sensor was made by FR-4 PCB, and the dimension was 2 mm × 3 mm × 1 mm. After adhesive was dropped in the DEA sensor heated at 280 °C, the dielectric loss factor was measured using an impedance analyzer (E4991A from Agilent) at 1 MHz for 1 min. The variation of dielectric loss measured from the impedance analyzer is shown in Figure 1. The curing time of NCA by DEA was measured twice per condition.

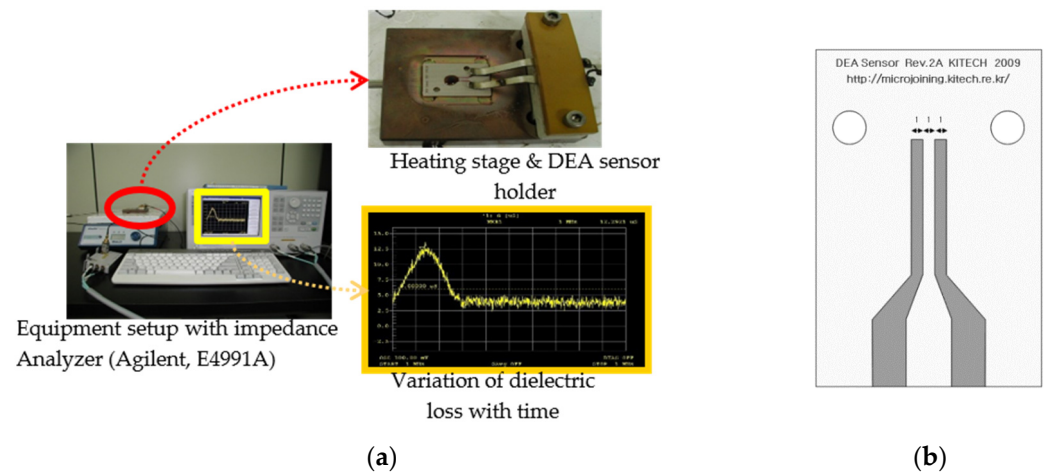


Figure 1. DEA measurement (a) equipment setup with impedance Analyzer, heating stage and DEA sensor, and variation of dielectric loss and (b) DEA sensor.

Dielectric data measured by the impedance analyzer can be expressed as dielectric constant, ϵ^* , and the equation can be expressed as

$$\epsilon^* = \epsilon' - i \epsilon'' \quad (1)$$

where ϵ' is the bulk permittivity, ϵ'' is the bulk loss factor, and i is $\sqrt{-1}$.

ϵ' can measure the polarization of the adhesive, and ϵ'' is related to the energy loss and the conductive nature of the adhesive. ϵ'' can be expressed as a parameter showing the dielectric loss factor because ϵ'' is directly proportional to the dielectric loss factor when conditions, such as frequency, time, temperature, etc., are fixed [17,24].

In this study, curing time was measured when the degree of cure reached 80 % [17]. Deviation of a cumulative line of dielectric loss curve was calculated, and two inflection points were considered as curing start and completion points. In the previous study [17], DEA-based curing time measurements were verified to be compatible with the DSC method.

2.2.2. Shear Strength Measurement

The shear strength of adhesive was measured using the die shear test. Specimens were made of an FR-4 PCB without solder resist and a dummy chip. The dimension of the PCB was 132 mm × 30 mm × 0.5 mm, and the dimension of the chip was 5.3 mm × 7.3 mm × 0.7 mm. Before flip-chip bonding, the PCB and chip were cleaned in a microwave plasma machine (TePla 660, PVA Tepla, Wettenberg, Germany). Adhesives were applied to the FR-4 PCB, and the thickness between the PCB and the dummy chip was evenly maintained using a 100 µm-thick polyimide film.

The thermo-compression bonding process was conducted using a flip-chip bonder (FCB-3, Panasonic, Osaka, Japan), and the thermos-profile is shown in Figure 2. The bonding process was conducted under a pre-heating temperature of 90 °C, a bonding temperature of 280 °C, a bonding time of 10 s, and a compression load of 100 N. The shear strength was measured using a bond tester (Dage BT-4000, Nordson, Manchester, UK) with a test load of 100 kg, a land speed of 167 µm, a shear height of 75 µm, and an overtravel of 100 µm. The shear strength was measured twice per condition.

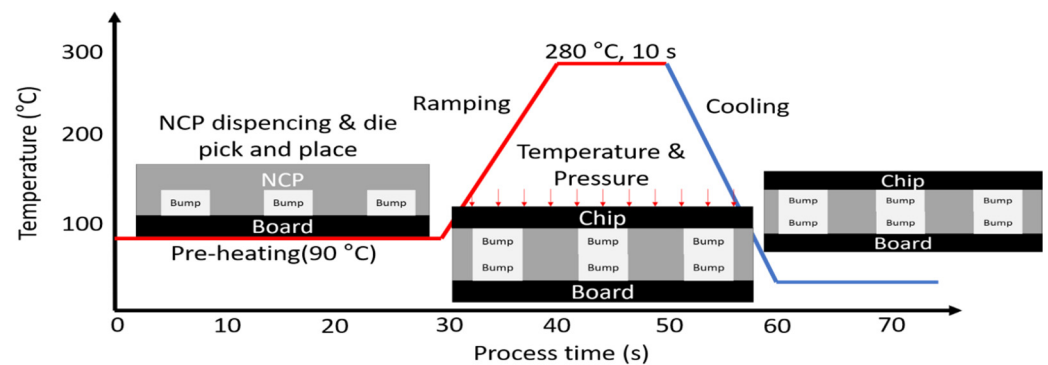


Figure 2. NCP flip-chip bonding process.

2.3. Neural Network Model

In this study, an artificial neural network (ANN) black-box model was selected to consider complex nonlinear relationships among numerous variables [25–27]. To build a prediction model, experimental datapoints for a curing time at 280 °C and shear strength at room temperature were predicted as stated in the previous section.

The input parameters are 4 types of resins, 2 types of hardeners, 8 types of catalysts, and a coupling agent, and 65 datapoints were used for the prediction of the curing time with regression models. 4 types of resins, 4 types of hardeners, 6 types of catalysts, and a coupling agent were used as input parameters, and 44 datapoints were used for the prediction of shear strength with regression models. The data sets for the curing time and the shear strength of NCA were listed in Appendix A.

The ANN model, as a multilayer perceptron (MLP) network, with one hidden layer with 3 nodes was used. In the hidden layer nodes, a rectified linear unit (ReLU) activation function was employed. An MSE loss function and adaptive moment estimation (ADAM) optimizer, which had a learning rate of 0.001, $\beta_1 = 0.9$, $\beta_2 = 0.999$, and $\epsilon = 10^{-8}$, were selected in model training and optimization. Modeling was implemented by Python and Keras application programming interfaces [28].

65 datapoints for the prediction of the curing time of NCA and 44 datapoints for the prediction of the shear strength of NCA were randomly divided into training and validation datasets at a ratio of 80 % and 20 %. Since the dataset is small and overfitting was not found in the model training, the model test step was omitted, and the model was verified using the third-party data which was not engaged in the training. The model was trained for 1000 epochs with minibatches of 10.

3. Results

3.1. Regression Models

In this study, the curing time and shear strength models were trained without overfitting as shown in Figure 3. The loss for the training set and the loss for the validation set decreased with each epoch number, and both loss datasets were converged after the 600th epoch.

The calculated MAEs and MAPEs for training and validation datasets for curing time and shear strength models were shown in Table 2. The MAEs for the training and validation datasets for the curing time model were 1.57 s and 1.84 s, respectively. The MAEs for the training and validation datasets for the shear strength were 6.08 MPa and 6.13 MPa, respectively. The MAPEs for the training and validation datasets for the curing time were 24.7 % and 25.4 %, respectively. The MAPEs for the training and validation datasets for the shear strength were 18.8 % and 22.5 %, respectively.

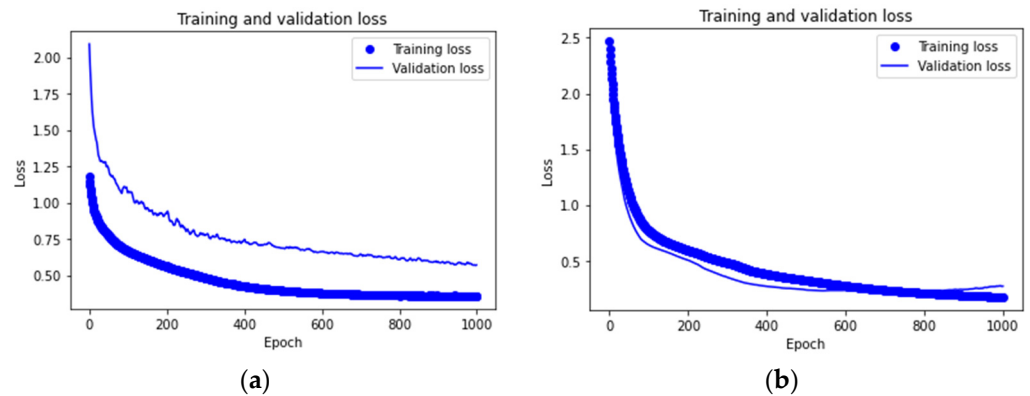


Figure 3. Training and validation losses for (a) curing time of NCA and (b) shear strength of NCA.

Table 2. Mean absolute error (MAE) and mean absolute percentage error (MAPE) of the trained models.

	MAE		MAPE	
	Curing Time (s)	Shear Strength (MPa)	Curing Time (%)	Shear Strength (%)
Training data set	1.57	6.08	24.7	18.8
Validation data set	1.84	6.13	25.4	22.5

The measured and predicted data were compared in Figures 4 and 5. The R^2 of training, validation, and all datasets for the curing time model were 0.61, 0.66, and 0.62, respectively. The R^2 of training, validation, and all datasets for the shear strength model were 0.85, 0.56, and 0.81, respectively.

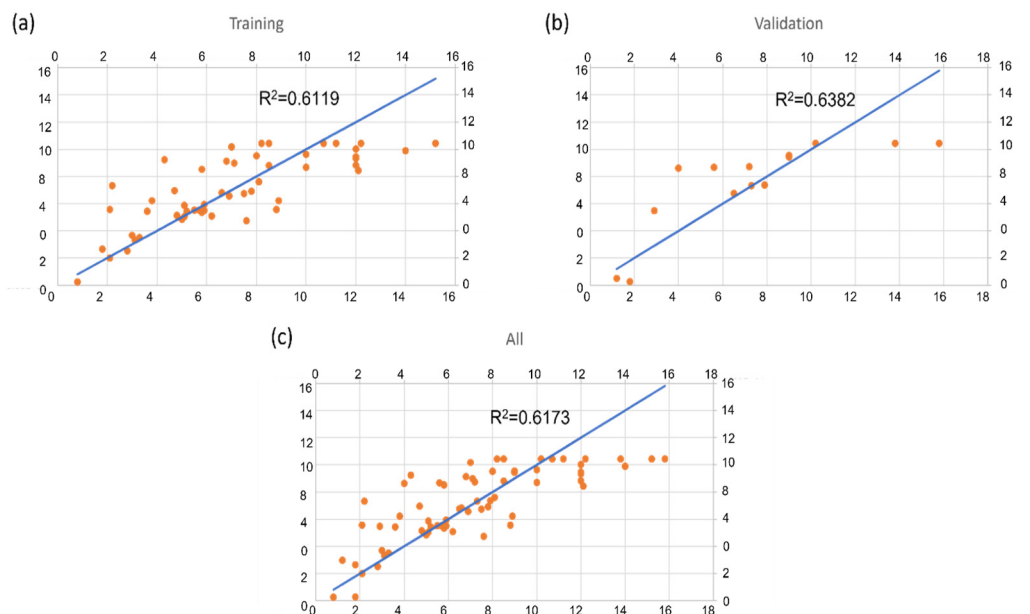


Figure 4. Correlation analysis for regression models for curing time of NCA (a) training, (b) validation, and (c) all.

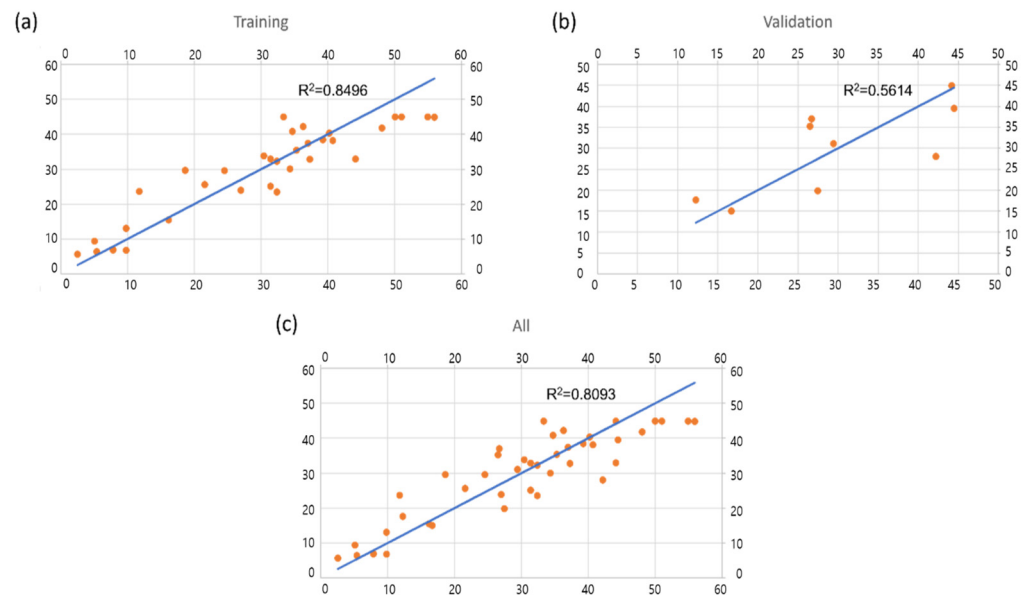


Figure 5. Correlation analysis for regression models for shear strength of NCA (a) training, (b) validation, and (c) all.

The curing time model has relatively low accuracy due to limited number of datapoints. Therefore, the model demonstrates a framework, but it is difficult to practically apply to the industry. The shear strength model showed better accuracy. Compared to Kang et al.'s research [23], they suggested R^2 of 0.64 for the shear strength prediction model. In this study, the accuracy of the shear strength is 28.9%–35.2% higher than their study. By increasing the number of datapoints, the accuracy of the regression models will be enhanced.

3.2. Verification of Curing Time and Shear Strength Using Third-Party Experimental Data

To verify the accuracy of the trained ANN models, the predicted curing time and the shear strength of NCA were compared with third-party experimental data. NCA formulation with 100 phr and 50 phr of DGEBA as the resin, 80 phr of MHHPA as the hardener, 15 phr of 2MZ as the catalyst, and 0.55 phr of coupling agent was selected to verify the curing time of NCA from Kim et al.'s study [4] and Min et al.'s study [20]. In order to verify the shear strength, NCA formulation, which is 50 phr of DGEBA, 80 phr of MHHPA, 20 phr of HX-3941, and 0.55 phr of coupling agent was selected from Kim et al. [29]'s study.

The predicted curing times from the trained ANN model were 3.9 s with 100 phr of the resin and 4.4 s with 50 phr of the resin, and the curing times from the reference [4,20] were 4.6 s and 4.0 s, respectively. The difference between the predicted and measured data were 0.7 s and 0.4 s, which can be accepted by using an adequate margin in the process design.

The predicted shear strength was 37.96 MPa, and the experimental shear strength for verification was 32.30 MPa [29]. The difference is relatively critical because the shear strength requirement of epoxy resin adhesive is 34.33 MPa [30,31]. The comparison is summarized in Table 3.

Table 3. Predicted and verified data of curing time and shear strength.

	Curing Time (s)		Shear Strength (MPa)
	[20]	[4]	[25]
Predicted data	3.9	4.4	37.96
Experimental data	4.6	4.0	32.30

3.3. Case Study 1: Prediction of Curing Time and Shear Strength of NCA Based on Resin, Hardener, and Catalyst Contents

The effects of input parameters on curing time and shear strength were investigated by the ANN models. In the estimation, curing time and shear strength were predicted by varying two input variables, while other variables were fixed.

Figure 6 shows the estimation of curing time according to the contents of resin and catalyst. DGEBA was considered as the resin, while HX-3941 and 2MZ were selected as the catalyst, respectively in Figure 6a,b. The hardener and the coupling agent were 80 phr of MHHPA and 0.55 phr of A-174, respectively. The curing times of NCA with HX-3941 and 2MZ catalyst were decreased from 8.19 s to 2.19 s and from 7.2 s to 3.9 s as the contents of resins and catalysts were increased. The increase in the content of the catalyst increases the number of reactors and the catalyst concentration [4,9,20], which resulted in a decreased curing time.

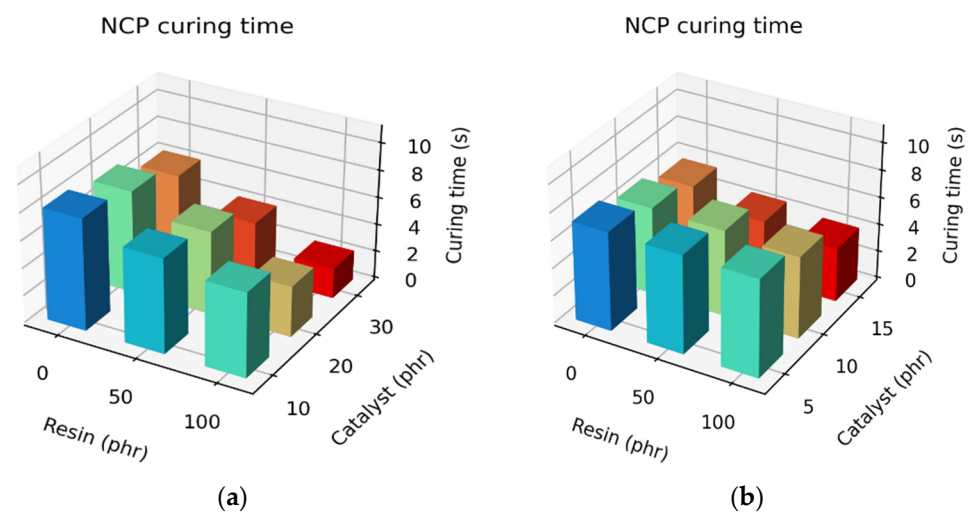


Figure 6. The predicted curing time with DGEBA (resin) (a) with HX-3941 (catalyst) and (b) with 2MZ (catalyst).

Figure 7 shows the estimation of shear strength according to the contents of resin and catalyst. DGEBA and HX-3941 were considered as the resin and the catalyst, respectively. The coupling agent was 0.55 phr of A-174, and 80 phr of MHHPA hardener was added (Figure 7a) or not (Figure 7b). The shear strengths with and without the hardener were predicted from 29.73 MPa to 45.52 MPa and from 13.97 MPa to 34.87 MPa, respectively. By increasing the catalyst content, the shear strength increased due to an increase in the number of reactors and the catalyst concentration. The predicted shear strength of NCA with the hardener showed 30.5–187% higher than that of NCA without the hardener. The role of the hardener is to cure the epoxy resin. The hardener causes a reaction with the epoxy groups, and the reaction creates a cross-linked polymer and prompts a strong chemical bonding mechanism [4,9,20,32].

Shear strength of 34.33 MPa or higher is recommended for commercial NCA with epoxy resin [30,31]. The predicted shear strengths of NCAs with the hardener were over 34.33 MPa when the resin content was more than 50 phr, and the catalyst content was more than 20 phr. However, the shear strengths of NCA without the hardener were lower than 34.33 MPa except for the 100 phr resin/30 phr catalyst case.

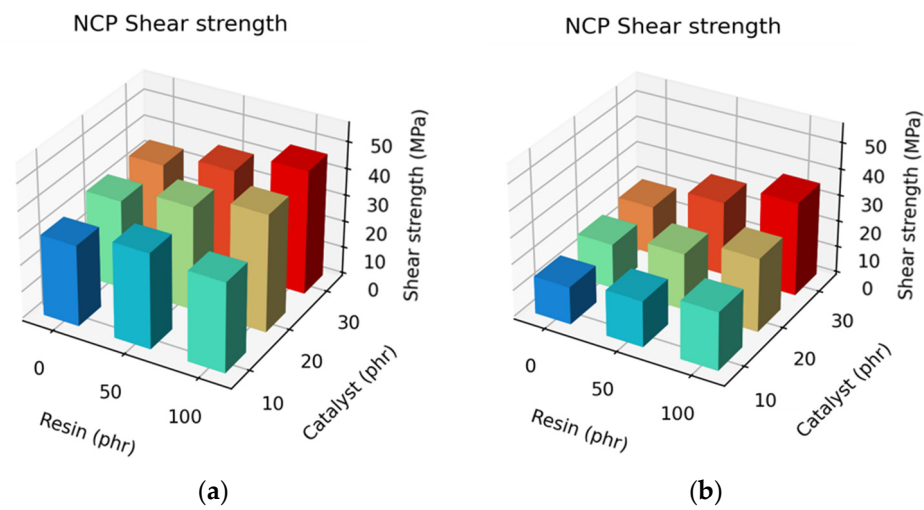


Figure 7. The predicted shear strength with DGEBA (resin) and HX-3941 (catalyst) (a) with hardener and (b) without hardener.

3.4. Case Study 2: Optimization of NCA Based on Resin, Hardener, and Catalyst

The snap curing time of fewer than 5 s and the shear strength of over 34.33 MPa of NCA are recommended to apply for mass production in the electronic industries [4,30,31]. NCA formulations satisfying the requirements were derived from the ANN models. In the optimization, the resin (DGEBA) and the catalyst (HX-3941) contents were used as input variables, while the hardener (MHHPA) and coupling agent (A-174) contents were fixed at 80 phr and 0.55 phr, respectively.

As shown in Figure 8, the optimized NCA formulations that satisfied conditions for mass production were shown using contours. The contours for curing time (s) were indicated as color, and the contours for shear strength (MPa) were indicated as a line.

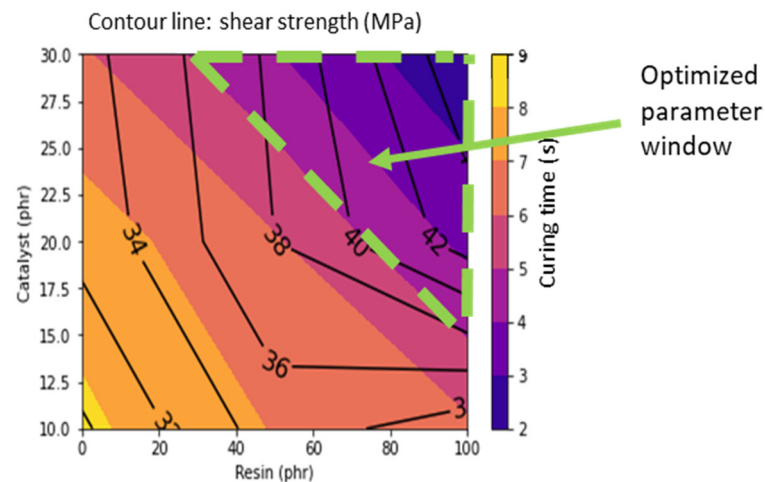


Figure 8. The optimized NCA formulation. Curing time (s) is contoured by color, and shear strength (MPa) is contoured by line.

The range of the optimized NCA satisfying both the curing time of fewer than 5 s and the shear strength of over 34.33 MPa was able to be approximated as a linear dotted line. The optimized NCA formulation was suggested as $0.2137 \times (\text{resin content in phr}) + (\text{catalyst content in phr}) \geq 35.87$. Increasing the resin content may reduce the required catalyst content and vice versa.

4. Conclusions

In this study, a framework for verification and prediction of the curing time/the shear strength of NCA and optimization of the NCA formulation using the ANN method was established. The snap curing time and the shear strength of NCA based on resin, hardener, catalyst, and coupling agent were modeled by ANN. The following conclusions were derived:

- (1) ANN models were constructed to predict the snap curing time and shear strength of NCA. The regression models indicated that the coefficients of determinations (R^2) were 28.9–35.2% higher accuracy in the prediction than the results of the reference even though only 65 datasets and 44 datasets were used in the ANN model.
- (2) In verifying the accuracy of the trained ANN models, the predicted curing time and shear strength from the trained ANN models were compared and verified with third-party experimental data. The predicted curing times and shear strength had errors of 0.3–0.7 s and 5.66 MPa, respectively.
- (3) The curing time and the shear strength in accordance with the content of resin, hardener, and catalyst were predicted. As the content of catalysts and resins was increased, the curing time was decreased, and the shear strength was also increased. In the combination of DGEBA resin, HX-3941 catalyst, 80 phr MHHPA hardener, and 0.55 phr A-174 coupling agent, the optimized NCA formulation was suggested the range of $0.2137 \times (\text{resin content in phr}) + (\text{catalyst content in phr}) \geq 35.87$ to meet mass production requirements.

This study proposed a neural network framework to predict the curing time/the shear strength and optimize NCA formulation based on epoxy resins, anhydride hardeners, imidazole and amine catalysts, and silane coupling agent. In the future research, polyurethane and polyamide resins will be considered, and data mining will be implementing using matching hardeners, catalysts, and coupling agents. In addition, in order to generalize the developed neural network model, it is necessary to develop characteristic indices including chemical chain length and reaction that can characterize polymer components.

Author Contributions: Conceptualization, K.-E.M., S.Y. and C.K.; methodology, K.-E.M., J.-W.J. and J.-K.K.; investigation, K.-E.M. and J.-W.J.; writing—original draft preparation, K.-E.M.; writing—review and editing, C.K. and S.Y.; project administration, C.K. All authors have read and agreed to the published version of the manuscript.

Funding: This study has been conducted with the support of the Korea Institute of Industrial Technology as “Development of root technology of multi-product flexible production (KITECH-EO-22-0006)”.

Institutional Review Board Statement: Not applicable.

Informed Consent Statement: Not applicable.

Data Availability Statement: The data presented in this study are available on request from the corresponding author.

Conflicts of Interest: The authors declare no conflict of interest.

Appendix A

The datapoints for the prediction of the curing time and the shear strength of NCA were listed in Tables [A1](#) and [A2](#).

Table A1. Data set for curing time of NCA.

DGEBA	DGEBF	Resin 160	ERL 4221	MHHPA	THPA	HX 3941	Z	2MZ	2E4MZ	2E4MZ-CN	2MZ-A	DICY	TPP	174	CT *
0	0	100	0	80	0	10	0	0	0	0	0	0	0	0.55	4.8
0	90	0	10	80	0	10	0	0	0	0	0	0	0	0.55	5.9
0	80	0	20	80	0	10	0	0	0	0	0	0	0	0.55	5.2
0	50	50	0	80	0	10	0	0	0	0	0	0	0	0.55	5.8
50	50	0	0	80	0	10	0	0	0	0	0	0	0	0.55	6.6
100	0	0	0	80	0	10	0	0	0	0	0	0	0	0.55	5.8
0	100	0	0	80	0	10	0	0	0	0	0	0	0	0.55	2.1
0	100	0	0	80	0	20	0	0	0	0	0	0	0	0.55	1.8
0	100	0	0	80	0	30	0	0	0	0	0	0	0	0.55	0.8
0	100	0	0	80	0	0	5	0	0	0	0	0	0	0.55	6.5
0	100	0	0	80	0	0	10	0	0	0	0	0	0	0.55	5.1
0	100	0	0	80	0	0	15	0	0	0	0	0	0	0.55	3.1
0	100	0	0	80	0	0	0	5	0	0	0	0	0	0.55	8.5
0	100	0	0	80	0	0	0	10	0	0	0	0	0	0.55	5.5
0	100	0	0	80	0	0	0	15	0	0	0	0	0	0.55	2.1
0	100	0	0	80	0	0	0	0	5	0	0	0	0	0.55	8.1
0	100	0	0	80	0	0	0	0	10	0	0	0	0	0.55	7.5
0	100	0	0	80	0	0	0	0	15	0	0	0	0	0.55	5.1
0	100	0	0	80	0	0	0	0	0	5	0	0	0	0.55	15.2
0	100	0	0	80	0	0	0	0	0	10	0	0	0	0.55	13.8
0	100	0	0	80	0	0	0	0	0	15	0	0	0	0.55	10.2
0	100	0	0	0	0	0	5	0	0	0	0	0	0	0.55	15.8
0	100	0	0	0	0	0	10	0	0	0	0	0	0	0.55	11.2
0	100	0	0	0	0	0	15	0	0	0	0	0	0	0.55	7.2
0	100	0	0	0	0	0	0	5	0	0	0	0	0	0.55	8.5
0	100	0	0	0	0	0	0	10	0	0	0	0	0	0.55	7.9
0	100	0	0	0	0	0	0	15	0	0	0	0	0	0.55	3.3
0	100	0	0	0	0	0	0	0	5	0	0	0	0	0.55	12.2
0	100	0	0	0	0	0	0	0	10	0	0	0	0	0.55	10.7
0	100	0	0	0	0	0	0	0	15	0	0	0	0	0.55	8.2
100	0	0	0	0	0	0	0	0	0	0	15	0	0	0.55	1.8
100	0	0	0	0	0	0	0	15	0	0	0	0	0	0.55	1.2
100	0	0	0	0	0	0	0	0	0	15	0	0	0	0.55	5.9
0	100	0	0	0	80	10	0	0	0	0	0	0	0	0.64	5.0
0	100	0	0	0	80	20	0	0	0	0	0	0	0	0.59	3.0
0	100	0	0	0	80	30	0	0	0	0	0	0	0	0.54	2.8
50	50	0	0	0	0	0	0	0	0	0	6.5	0	0	0.55	2.2
50	50	0	0	0	0	0	0	0	0	0	7	0	0	0.55	4.7
50	50	0	0	0	0	0	0	0	0	0	8	0	0	0.55	3.8
50	50	0	0	0	0	0	0	0	0	0	9	0	0	0.55	2.9
50	50	0	0	0	0	0	0	0	0	0	5	0	0	0.55	12.1
50	50	0	0	0	0	0	0	0	0	0	5	0	0	0.55	5.8
50	50	0	0	0	0	0	0	0	0	0	5	2	0	0.55	5.8
50	50	0	0	0	0	0	0	0	0	0	5	2	1	0.55	4.3
50	50	0	0	0	0	0	0	0	0	0	5	0	0	0.55	6.8
50	50	0	0	0	0	0	0	0	0	0	5	1	0.5	0.55	12.0
50	50	0	0	0	0	0	0	0	0	0	5	4	0.5	0.55	7.1
50	50	0	0	0	0	0	0	0	0	0	5	1	2	0.55	14.0
50	50	0	0	0	0	0	0	0	0	0	5	4	2	0.55	12.0
50	50	0	0	0	0	0	0	0	0	0	5	0.38	1.25	0.55	12.0
50	50	0	0	0	0	0	0	0	0	0	5	4.62	1.25	0.55	8.0
50	50	0	0	0	0	0	0	0	0	0	5	2.5	0.19	0.55	10.0
50	50	0	0	0	0	0	0	0	0	0	5	2.5	2.31	0.55	7.0
50	50	0	0	0	0	0	0	0	0	0	5	2.5	1.25	0.55	9.0
50	50	0	0	0	0	0	0	0	0	0	6.5	0	0	0.55	7.3
50	50	0	0	0	0	0	0	0	0	0	5	4	0	0.55	4.0
50	50	0	0	0	0	0	0	0	0	0	4	6	0	0.55	12.0
50	50	0	0	0	0	0	0	0	0	0	4	8	0	0.55	9.0
50	50	0	0	0	0	0	0	0	0	0	4	10	0	0.55	10.0
50	50	0	0	0	0	0	0	0	0	0	8	0	0	0.55	8.9
50	50	0	0	0	0	0	0	0	0	0	10	0	0	0.55	7.6
50	50	0	0	0	0	0	0	0	0	0	8	0	0.5	0.55	6.9
50	50	0	0	0	0	0	0	0	0	0	8	0	1	0.55	7.8
50	50	0	0	0	0	0	0	0	0	0	10	0	0.5	0.55	6.2
50	50	0	0	0	0	0	0	0	0	0	10	0	1	0.55	3.6

* CT is curing time. Unit of CT is second, and units of others are phr.

Table A2. Data set for shear strength of NCA.

DGEBA	DGEBF	Resin 160	ERL 4221	MHHPA	THPA	M8T2 (MHHPA 80+THPA 20)	ADH	3941	Z	2MZ	2E4MZ	2E4MZ_CN	2MZ_A	174	SS *
0	0	100	0	80	0	0	0	10	0	0	0	0	0	0.55	51.01
0	90	0	10	80	0	0	0	10	0	0	0	0	0	0.55	26.48
0	80	0	20	80	0	0	0	10	0	0	0	0	0	0.55	40.22
0	50	50	0	80	0	0	0	10	0	0	0	0	0	0.55	33.35
50	50	0	0	80	0	0	0	10	0	0	0	0	0	0.55	36.29
100	0	0	0	80	0	0	0	10	0	0	0	0	0	0.55	32.37
0	100	0	0	80	0	0	0	10	0	0	0	0	0	0.55	34.33
50	50	0	0	90	10	0	0	10	0	0	0	0	0	0.55	34.67
50	50	0	0	80	20	0	0	10	0	0	0	0	0	0.55	44.41
50	50	0	0	70	30	0	0	10	0	0	0	0	0	0.55	40.73
0	100	0	0	80	0	0	0	0	5	0	0	0	0	0.55	16.18
0	100	0	0	80	0	0	0	0	10	0	0	0	0	0.55	31.39
0	100	0	0	80	0	0	0	0	15	0	0	0	0	0.55	21.58
0	100	0	0	80	0	0	0	0	0	5	0	0	0	0.55	27.46
0	100	0	0	80	0	0	0	0	0	10	0	0	0	0.55	30.41
0	100	0	0	80	0	0	0	0	0	15	0	0	0	0.55	37.27
0	100	0	0	80	0	0	0	0	0	0	5	0	0	0.55	12.26
0	100	0	0	80	0	0	0	0	0	0	10	0	0	0.55	24.52
0	100	0	0	80	0	0	0	0	0	0	15	0	0	0.55	29.43
0	100	0	0	80	0	0	0	0	0	0	0	5	0	0.55	5.39
0	100	0	0	80	0	0	0	0	0	0	0	10	0	0.55	7.84
0	100	0	0	80	0	0	0	0	0	0	0	15	0	0.55	9.81
0	100	0	0	0	0	0	0	0	5	0	0	0	0	0.55	11.77
0	100	0	0	0	0	0	0	0	10	0	0	0	0	0.55	44.14
0	100	0	0	0	0	0	0	0	15	0	0	0	0	0.55	31.39
0	100	0	0	0	0	0	0	0	0	5	0	0	0	0.55	18.63
0	100	0	0	0	0	0	0	0	0	10	0	0	0	0.55	55.91
0	100	0	0	0	0	0	0	0	0	15	0	0	0	0.55	50.03
0	100	0	0	0	0	0	0	0	0	0	5	0	0	0.55	42.18
0	100	0	0	0	0	0	0	0	0	0	10	0	0	0.55	48.06
0	100	0	0	0	0	0	0	0	0	0	15	0	0	0.55	54.93
0	100	0	0	0	0	0	0	0	0	0	0	10	0	0.55	5.10
0	100	0	0	0	0	0	0	0	0	0	0	15	0	0.55	7.84
100	0	0	0	0	0	0	0	0	0	0	0	0	15	0.55	2.53
0	100	0	0	0	0	0	0	20	0	0	0	0	0	0.59	16.67
0	100	0	0	0	0	0	0	30	0	0	0	0	0	0.54	44.14
50	50	0	0	0	0	0	3.75	0	0	0	0	0	15	0.55	35.27
50	50	0	0	0	0	0	7.5	0	0	0	0	0	15	0.55	37.01
50	50	0	0	0	0	0	11.25	0	0	0	0	0	15	0.55	39.26
50	50	0	0	0	0	0	15	0	0	0	0	0	15	0.55	26.72
50	50	0	0	0	0	80	0	0	0	15	0	0	0	0.55	9.81
50	50	0	0	0	0	80	0	0	0	0	0	0	15	0.55	26.97
50	50	0	0	0	0	0	23	0	0	0	0	0	15	0.55	32.37

* SS is shear strength. Unit of SS is MPa, and units of others are phr.

References

1. Yim, M.J.; Paik, K.W. Review of electrically conductive adhesive technologies for electronic packaging. *Electron. Mater. Lett.* **2006**, *2*, 183–194.
2. Tong, X.C. Characterization methodologies of thermal management materials. In *Advanced Materials for Thermal Management of Electronic Packaging*; Springer: New York, NY, USA, 2011; pp. 59–129.
3. Li, Y.; Wong, C. Recent advances of conductive adhesives as a lead-free alternative in electronic packaging: Materials, processing, reliability and applications. *Mater. Sci. Eng. R Rep.* **2006**, *51*, 1–35. [[CrossRef](#)]
4. Kim, H.-Y.; Min, K.-E.; Lee, J.-S.; Lee, S.-J.; Lee, S.-S.; Kim, J.-K. Reliability of an ultra-fine-pitch COF flip-chip package using non-conductive paste. *Electron. Mater. Lett.* **2016**, *12*, 48–53. [[CrossRef](#)]
5. Chiu, Y.; Chan, Y.; Lui, S. Study of short-circuiting between adjacent joints under electric field effects in fine pitch anisotropic conductive adhesive interconnects. *Microelectron. Reliab.* **2002**, *42*, 1945–1951. [[CrossRef](#)]
6. Lee, S.-M.; Kim, B.-G.; Kim, Y.-H. Non-conductive adhesive (NCA) trapping study in chip on glass joints fabricated using Sn bumps and NCA. *Mater. Trans.* **2008**, 0807280502. [[CrossRef](#)]
7. Back, J.-H.; Hwang, C.; Baek, D.; Kim, D.; Yu, Y.; Lee, W.; Kim, H.-J. Synthesis of urethane-modified aliphatic epoxy using a greenhouse gas for epoxy composites with tunable properties: Toughened polymer, elastomer, and pressure-sensitive adhesive. *Compos. Part B Eng.* **2021**, *222*, 109058. [[CrossRef](#)]
8. Charles, A.D.; Rider, A.N. Triblock copolymer toughening of a carbon fibre-reinforced epoxy composite for bonded repair. *Polymer* **2018**, *10*, 888. [[CrossRef](#)]
9. Min, K.-E.; Kim, H.-Y.; Bang, J.-H.; Kim, J.-H.; Kim, J.-K. Effects of hardeners and catalysts on the reliability of copper to copper adhesive joint. *Korean J. Mater. Res.* **2011**, *21*, 283–287. [[CrossRef](#)]

10. Lee, T.-Y.; Kim, M.-S.; Ko, Y.-H.; Kim, Y.-H.; Yoo, S. Epoxy/silane pre-synthesis improving thermal properties and adhesion strength of silica-filled non-conductive adhesive for fine-pitch thermocompression bonding. *J. Mater. Sci. Mater. Electron.* **2020**, *31*, 1227–1235. [[CrossRef](#)]
11. Aradhana, R.; Mohanty, S.; Nayak, S.K. A review on epoxy-based electrically conductive adhesives. *Int. J. Adhes. Adhes.* **2020**, *99*, 102596. [[CrossRef](#)]
12. Zhang, S.; Qi, X.; Yang, M.; Cao, Y.; Lin, T.; He, P.; Paik, K.-W. A study on the resistivity and mechanical properties of modified nano-Ag coated Cu particles in electrically conductive adhesives. *J. Mater. Sci. Mater. Electron.* **2019**, *30*, 9171–9183. [[CrossRef](#)]
13. Aradhana, R.; Mohanty, S.; Nayak, S.K. High performance electrically conductive epoxy/reduced graphene oxide adhesives for electronics packaging applications. *J. Mater. Sci. Mater. Electron.* **2019**, *30*, 4296–4309. [[CrossRef](#)]
14. Lopes, P.; Moura, D.; Freitas, D.; Proença, M.; Figueiredo, H.; Alves, R.; Paiva, M. Advanced electrically conductive adhesives for high complexity PCB assembly. *AIP Conf. Proc.* **2019**, *2055*, 090009.
15. Wang, X.-Q.; Gan, W.-P.; Xiang, F.; Li, B.-Y. Effect of curing agent and curing substrate on low temperature curable silver conductive adhesive. *J. Mater. Sci. Mater. Electron.* **2019**, *30*, 2829–2836. [[CrossRef](#)]
16. Tsai, W.S.; Huang, C.; Chung, C.K.; Yu, K.; Lin, C. Generational changes of flip chip interconnection technology. In Proceedings of the 2017 12th International Microsystems, Packaging, Assembly and Circuits Technology Conference (IMPACT), Taipei, Taiwan, 25–27 October 2017; pp. 306–310.
17. Min, K.-E.; Lee, J.-S.; Lee, S.-J.; Yi, S.; Kim, J.-K. Evaluation method for snap cure behavior of non-conductive paste for flip chip bonding. *J. Weld. Jt.* **2015**, *33*, 41–46. [[CrossRef](#)]
18. Roach, D.; Rackow, K.; Duvall, R. Innovative use of adhesive interface characteristics to nondestructively quantify the strength of bonded joints. In Proceedings of the 10th European Conference on Non-Destructive Testing, Moscow, Russia, 7–11 June 2010; pp. 7–11.
19. Lin, Y.-M.; Zhan, C.-J.; Kao, K.-S.; Fan, C.-W.; Chung, S.-C.; Huang, Y.-W.; Huang, S.-Y.; Chang, J.-Y.; Yang, T.-F.; Lau, J.H. Low temperature bonding using non-conductive adhesive for 3D chip stacking with 30 μ m-pitch micro solder bump interconnections. In Proceedings of the 2012 IEEE 62nd Electronic Components and Technology Conference, San Diego, CA, USA, 29 May–1 June 2012; pp. 1656–1661.
20. Min, K.-E.; Lee, J.-S.; Yoo, S.-H.; Kim, M.-S.; Kim, J.-K. Effects of catalysts on the adhesive properties for flip chip bonding. *Korean J. Mater. Res.* **2010**, *20*, 681–685. [[CrossRef](#)]
21. Yang, S.Y.; Lee, S.-B.; Kwon, W.-S.; Paik, K.-W. Analytical approach to evaluate shear stress in flip chip interconnection using NCA/ACF. In Proceedings of the 4th International Symposium on Electronic Materials and Packaging, 2002, Kaohsiung, Taiwan, 4–6 December 2002; pp. 204–209.
22. Pruksawan, S.; Lambard, G.; Samitsu, S.; Sodeyama, K.; Naito, M. Prediction and optimization of epoxy adhesive strength from a small dataset through active learning. *Sci. Technol. Adv. Mater.* **2019**, *20*, 1010–1021. [[CrossRef](#)] [[PubMed](#)]
23. Kang, H.; Lee, J.H.; Choe, Y.; Lee, S.G. Prediction of lap shear strength and impact peel strength of epoxy adhesive by machine learning approach. *Nanomaterials* **2021**, *11*, 872. [[CrossRef](#)]
24. He, Y. DSC and DEA studies of underfill curing kinetics. *Thermochim. Acta* **2001**, *367*, 101–106. [[CrossRef](#)]
25. Li, Y.; Lei, G.; Bramerdorfer, G.; Peng, S.; Sun, X.; Zhu, J. Machine Learning for Design Optimization of Electromagnetic Devices: Recent Developments and Future Directions. *Appl. Sci.* **2021**, *11*, 1627. [[CrossRef](#)]
26. Al-Shamiri, A.K.; Yuan, T.-F.; Kim, J.H. Non-Tuned Machine Learning Approach for Predicting the Compressive Strength of High-Performance Concrete. *Materials* **2020**, *13*, 1023. [[CrossRef](#)]
27. Mjalli, F.S.; Al-Asheh, S.; Alfadala, H. Use of artificial neural network black-box modeling for the prediction of wastewater treatment plants performance. *J. Environ. Manag.* **2007**, *83*, 329–338. [[CrossRef](#)]
28. Chollet, F. *Deep Learning with Python*; Manning Publications Co.: Shelter Island, NY, USA, 2018.
29. Kim, M.-S.; Kim, H.-Y.; Yoo, S.-H.; Kim, J.-H.; Kim, J.-K. Effect of curing agent on the curing behavior and joint strength of epoxy adhesive. *J. Weld. Jt.* **2011**, *29*, 54–60. [[CrossRef](#)]
30. Licari, J.J.; Swanson, D.W. *Adhesives Technology for Electronic Applications: Materials, Processing, Reliability*; William Andrew: Waltham, MA, USA, 2011.
31. George, K.; Thomas, A.; Shajimon, N.; Joseph, J.; Paul, R. A Review on Electrically Conductive Adhesives in Electronic Packaging. *Int. J. Res. Appl. Sci. Eng. Technol.* **2021**, *9*, 440–452. [[CrossRef](#)]
32. Choi, W.-J.; Yoo, S.-H.; Lee, H.-S.; Kim, M.-S.; Kim, J.-K. Effects of hardeners on the low-temperature snap cure behaviors of epoxy adhesives for flip chip bonding. *Korean J. Mater. Res.* **2012**, *22*, 454–458. [[CrossRef](#)]